

Study of the reaction $e^+e^- \rightarrow J/\psi \pi^+\pi^-$ via initial-state radiation at *BABAR*

J. P. Lees,¹ V. Poireau,¹ V. Tisserand,¹ J. Garra Tico,² E. Grauges,² A. Palano^{ab,3} G. Eigen,⁴ B. Stugu,⁴ D. N. Brown,⁵ L. T. Kerth,⁵ Yu. G. Kolomensky,⁵ G. Lynch,⁵ H. Koch,⁶ T. Schroeder,⁶ D. J. Asgeirsson,⁷ C. Hearty,⁷ T. S. Mattison,⁷ J. A. McKenna,⁷ A. Khan,⁸ V. E. Blinov,⁹ A. R. Buzykaev,⁹ V. P. Druzhinin,⁹ V. B. Golubev,⁹ E. A. Kravchenko,⁹ A. P. Onuchin,⁹ S. I. Serednyakov,⁹ Yu. I. Skovpen,⁹ E. P. Solodov,⁹ K. Yu. Todyshev,⁹ A. N. Yushkov,⁹ M. Bondioli,¹⁰ D. Kirkby,¹⁰ A. J. Lankford,¹⁰ M. Mandelkern,¹⁰ H. Atmacan,¹¹ J. W. Gary,¹¹ F. Liu,¹¹ O. Long,¹¹ G. M. Vitug,¹¹ C. Campagnari,¹² T. M. Hong,¹² D. Kovalskyi,¹² J. D. Richman,¹² C. A. West,¹² A. M. Eisner,¹³ J. Kroseberg,¹³ W. S. Lockman,¹³ A. J. Martinez,¹³ B. A. Schumm,¹³ A. Seiden,¹³ D. S. Chao,¹⁴ C. H. Cheng,¹⁴ B. Echenard,¹⁴ K. T. Flood,¹⁴ D. G. Hitlin,¹⁴ P. Ongmongkolkul,¹⁴ F. C. Porter,¹⁴ A. Y. Rakin,¹⁴ R. Andreassen,¹⁵ Z. Huard,¹⁵ B. T. Meadows,¹⁵ M. D. Sokoloff,¹⁵ L. Sun,¹⁵ P. C. Bloom,¹⁶ W. T. Ford,¹⁶ A. Gaz,¹⁶ U. Nauenberg,¹⁶ J. G. Smith,¹⁶ S. R. Wagner,¹⁶ R. Ayad,¹⁷ * W. H. Toki,¹⁷ B. Spaan,¹⁸ K. R. Schubert,¹⁹ R. Schwierz,¹⁹ D. Bernard,²⁰ M. Verderi,²⁰ P. J. Clark,²¹ S. Playfer,²¹ D. Bettoni^{a,22} C. Bozzi^{a,22} R. Calabrese^{ab,22} G. Cibinetto^{ab,22} E. Fioravanti^{ab,22} I. Garzia^{ab,22} E. Luppi^{ab,22} M. Munerato^{ab,22} M. Negrini^{ab,22} L. Piemontese^{a,22} V. Santoro^{a,22} R. Baldini-Ferrolì,²³ A. Calcaterra,²³ R. de Sangro,²³ G. Finocchiaro,²³ P. Patteri,²³ I. M. Peruzzi,^{23,†} M. Piccolo,²³ M. Rama,²³ A. Zallo,²³ R. Contri^{ab,24} E. Guido^{ab,24} M. Lo Vetere^{ab,24} M. R. Monge^{ab,24} S. Passaggio^{a,24} C. Patrignani^{ab,24} E. Robutti^{a,24} B. Bhuyan,²⁵ V. Prasad,²⁵ C. L. Lee,²⁶ M. Morii,²⁶ A. J. Edwards,²⁷ A. Adametz,²⁸ U. Uwer,²⁸ H. M. Lacker,²⁹ T. Lueck,²⁹ P. D. Dauncey,³⁰ P. K. Behera,³¹ U. Mallik,³¹ C. Chen,³² J. Cochran,³² W. T. Meyer,³² S. Prell,³² A. E. Rubin,³² A. V. Gritsan,³³ Z. J. Guo,³³ N. Arnaud,³⁴ M. Davier,³⁴ D. Derkach,³⁴ G. Grosdidier,³⁴ F. Le Diberder,³⁴ A. M. Lutz,³⁴ B. Malaescu,³⁴ P. Roudeau,³⁴ M. H. Schune,³⁴ A. Stocchi,³⁴ G. Wormser,³⁴ D. J. Lange,³⁵ D. M. Wright,³⁵ C. A. Chavez,³⁶ J. P. Coleman,³⁶ J. R. Fry,³⁶ E. Gabathuler,³⁶ D. E. Hutchcroft,³⁶ D. J. Payne,³⁶ C. Touramanis,³⁶ A. J. Bevan,³⁷ F. Di Lodovico,³⁷ R. Sacco,³⁷ M. Sigamani,³⁷ G. Cowan,³⁸ D. N. Brown,³⁹ C. L. Davis,³⁹ A. G. Denig,⁴⁰ M. Fritsch,⁴⁰ W. Gradl,⁴⁰ K. Griessinger,⁴⁰ A. Hafner,⁴⁰ E. Prencipe,⁴⁰ R. J. Barlow,^{41,‡} G. Jackson,⁴¹ G. D. Lafferty,⁴¹ E. Behn,⁴² R. Cenci,⁴² B. Hamilton,⁴² A. Jawahery,⁴² D. A. Roberts,⁴² C. Dallapiccola,⁴³ R. Cowan,⁴⁴ D. Dujmic,⁴⁴ G. Sciolla,⁴⁴ R. Cheaib,⁴⁵ D. Lindemann,⁴⁵ P. M. Patel,⁴⁵ S. H. Robertson,⁴⁵ P. Biassoni^{ab,46} N. Neri^{a,46} F. Palombo^{ab,46} S. Stracka^{ab,46} L. Cremaldi,⁴⁷ R. Godang,^{47,§} R. Kroeger,⁴⁷ P. Sonnek,⁴⁷ D. J. Summers,⁴⁷ X. Nguyen,⁴⁸ M. Simard,⁴⁸ P. Taras,⁴⁸ G. De Nardo^{ab,49} D. Monorchio^{ab,49} G. Onorato^{ab,49} C. Sciacca^{ab,49} M. Martinelli,⁵⁰ G. Raven,⁵⁰ C. P. Jessop,⁵¹ J. M. LoSecco,⁵¹ W. F. Wang,⁵¹ K. Honscheid,⁵² R. Kass,⁵² J. Brau,⁵³ R. Frey,⁵³ N. B. Sinev,⁵³ D. Strom,⁵³ E. Torrence,⁵³ E. Feltresi^{ab,54} N. Gagliardi^{ab,54} M. Margoni^{ab,54} M. Morandin^{a,54} M. Posocco^{a,54} M. Rotondo^{a,54} G. Simi^{a,54} F. Simonetto^{ab,54} R. Stroili^{ab,54} S. Akar,⁵⁵ E. Ben-Haim,⁵⁵ M. Bomben,⁵⁵ G. R. Bonneaud,⁵⁵ H. Briand,⁵⁵ G. Calderini,⁵⁵ J. Chauveau,⁵⁵ O. Hamon,⁵⁵ Ph. Leruste,⁵⁵ G. Marchiori,⁵⁵ J. Ocariz,⁵⁵ S. Sitt,⁵⁵ M. Biasini^{ab,56} E. Manoni^{ab,56} S. Pacetti^{ab,56} A. Rossi^{ab,56} C. Angelini^{ab,57} G. Batignani^{ab,57} S. Bettarini^{ab,57} M. Carpinelli^{ab,57,¶} G. Casarosa^{ab,57} A. Cervelli^{ab,57} F. Forti^{ab,57} M. A. Giorgi^{ab,57} A. Lusiani^{ac,57} B. Oberhof^{ab,57} E. Paoloni^{ab,57} A. Perez^{a,57} G. Rizzo^{ab,57} J. J. Walsh^{a,57} D. Lopes Pegna,⁵⁸ J. Olsen,⁵⁸ A. J. S. Smith,⁵⁸ A. V. Telnov,⁵⁸ F. Anulli^{a,59} R. Faccini^{ab,59} F. Ferrarotto^{a,59} F. Ferroni^{ab,59} M. Gaspero^{ab,59} L. Li Gioi^{a,59} M. A. Mazzoni^{a,59} G. Piredda^{a,59} C. Büniger,⁶⁰ O. Grünberg,⁶⁰ T. Hartmann,⁶⁰ T. Leddig,⁶⁰ H. Schröder,⁶⁰ C. Voss,⁶⁰ R. Waldi,⁶⁰ T. Adye,⁶¹ E. O. Olaiya,⁶¹ F. F. Wilson,⁶¹ S. Emery,⁶² G. Hamel de Monchenault,⁶² G. Vasseur,⁶² Ch. Yèche,⁶² D. Aston,⁶³ D. J. Bard,⁶³ R. Bartoldus,⁶³ J. F. Benitez,⁶³ C. Cartaro,⁶³ M. R. Convery,⁶³ J. Dorfan,⁶³ G. P. Dubois-Felsmann,⁶³ W. Dunwoodie,⁶³ M. Ebert,⁶³ R. C. Field,⁶³ M. Franco Sevilla,⁶³ B. G. Fulsom,⁶³ A. M. Gabareen,⁶³ M. T. Graham,⁶³ P. Grenier,⁶³ C. Hast,⁶³ W. R. Innes,⁶³ M. H. Kelsey,⁶³ P. Kim,⁶³ M. L. Kocian,⁶³ D. W. G. S. Leith,⁶³ P. Lewis,⁶³ B. Lindquist,⁶³ S. Luitz,⁶³ V. Luth,⁶³ H. L. Lynch,⁶³ D. B. MacFarlane,⁶³ D. R. Muller,⁶³ H. Neal,⁶³ S. Nelson,⁶³ M. Perl,⁶³ T. Pulliam,⁶³ B. N. Ratcliff,⁶³ A. Roodman,⁶³ A. A. Salnikov,⁶³ R. H. Schindler,⁶³ A. Snyder,⁶³ D. Su,⁶³ M. K. Sullivan,⁶³ J. Va'vra,⁶³ A. P. Wagner,⁶³ W. J. Wisniewski,⁶³ M. Wittgen,⁶³ D. H. Wright,⁶³ H. W. Wulsin,⁶³ C. C. Young,⁶³ V. Ziegler,⁶³ W. Park,⁶⁴ M. V. Purohit,⁶⁴ R. M. White,⁶⁴ J. R. Wilson,⁶⁴ A. Randle-Conde,⁶⁵ S. J. Sekula,⁶⁵ M. Bellis,⁶⁶ P. R. Burchat,⁶⁶ T. S. Miyashita,⁶⁶ M. S. Alam,⁶⁷ J. A. Ernst,⁶⁷ R. Gorodeisky,⁶⁸ N. Guttman,⁶⁸ D. R. Peimer,⁶⁸ A. Soffer,⁶⁸ P. Lund,⁶⁹ S. M. Spanier,⁶⁹ J. L. Ritchie,⁷⁰ A. M. Ruland,⁷⁰ R. F. Schwitters,⁷⁰ B. C. Wray,⁷⁰ J. M. Izen,⁷¹

X. C. Lou,⁷¹ F. Bianchi^{ab,72} D. Gamba^{ab,72} L. Lanceri^{ab,73} L. Vitale^{ab,73} F. Martinez-Vidal,⁷⁴ A. Oyanguren,⁷⁴ H. Ahmed,⁷⁵ J. Albert,⁷⁵ Sw. Banerjee,⁷⁵ F. U. Bernlochner,⁷⁵ H. H. F. Choi,⁷⁵ G. J. King,⁷⁵ R. Kowalewski,⁷⁵ M. J. Lewczuk,⁷⁵ I. M. Nugent,⁷⁵ J. M. Roney,⁷⁵ R. J. Sobie,⁷⁵ N. Tasneem,⁷⁵ T. J. Gershon,⁷⁶ P. F. Harrison,⁷⁶ T. E. Latham,⁷⁶ E. M. T. Puccio,⁷⁶ H. R. Band,⁷⁷ S. Dasu,⁷⁷ Y. Pan,⁷⁷ R. Prepost,⁷⁷ and S. L. Wu⁷⁷

(The BABAR Collaboration)

¹Laboratoire d'Annecy-le-Vieux de Physique des Particules (LAPP),
Université de Savoie, CNRS/IN2P3, F-74941 Annecy-Le-Vieux, France

²Universitat de Barcelona, Facultat de Física, Departament ECM, E-08028 Barcelona, Spain

³INFN Sezione di Bari^a; Dipartimento di Fisica, Università di Bari^b, I-70126 Bari, Italy

⁴University of Bergen, Institute of Physics, N-5007 Bergen, Norway

⁵Lawrence Berkeley National Laboratory and University of California, Berkeley, California 94720, USA

⁶Ruhr Universität Bochum, Institut für Experimentalphysik 1, D-44780 Bochum, Germany

⁷University of British Columbia, Vancouver, British Columbia, Canada V6T 1Z1

⁸Brunel University, Uxbridge, Middlesex UB8 3PH, United Kingdom

⁹Budker Institute of Nuclear Physics, Novosibirsk 630090, Russia

¹⁰University of California at Irvine, Irvine, California 92697, USA

¹¹University of California at Riverside, Riverside, California 92521, USA

¹²University of California at Santa Barbara, Santa Barbara, California 93106, USA

¹³University of California at Santa Cruz, Institute for Particle Physics, Santa Cruz, California 95064, USA

¹⁴California Institute of Technology, Pasadena, California 91125, USA

¹⁵University of Cincinnati, Cincinnati, Ohio 45221, USA

¹⁶University of Colorado, Boulder, Colorado 80309, USA

¹⁷Colorado State University, Fort Collins, Colorado 80523, USA

¹⁸Technische Universität Dortmund, Fakultät Physik, D-44221 Dortmund, Germany

¹⁹Technische Universität Dresden, Institut für Kern- und Teilchenphysik, D-01062 Dresden, Germany

²⁰Laboratoire Leprince-Ringuet, Ecole Polytechnique, CNRS/IN2P3, F-91128 Palaiseau, France

²¹University of Edinburgh, Edinburgh EH9 3JZ, United Kingdom

²²INFN Sezione di Ferrara^a; Dipartimento di Fisica, Università di Ferrara^b, I-44100 Ferrara, Italy

²³INFN Laboratori Nazionali di Frascati, I-00044 Frascati, Italy

²⁴INFN Sezione di Genova^a; Dipartimento di Fisica, Università di Genova^b, I-16146 Genova, Italy

²⁵Indian Institute of Technology Guwahati, Guwahati, Assam, 781 039, India

²⁶Harvard University, Cambridge, Massachusetts 02138, USA

²⁷Harvey Mudd College, Claremont, California 91711

²⁸Universität Heidelberg, Physikalisches Institut, Philosophenweg 12, D-69120 Heidelberg, Germany

²⁹Humboldt-Universität zu Berlin, Institut für Physik, Newtonstr. 15, D-12489 Berlin, Germany

³⁰Imperial College London, London, SW7 2AZ, United Kingdom

³¹University of Iowa, Iowa City, Iowa 52242, USA

³²Iowa State University, Ames, Iowa 50011-3160, USA

³³Johns Hopkins University, Baltimore, Maryland 21218, USA

³⁴Laboratoire de l'Accélérateur Linéaire, IN2P3/CNRS et Université Paris-Sud 11,
Centre Scientifique d'Orsay, B. P. 34, F-91898 Orsay Cedex, France

³⁵Lawrence Livermore National Laboratory, Livermore, California 94550, USA

³⁶University of Liverpool, Liverpool L69 7ZE, United Kingdom

³⁷Queen Mary, University of London, London, E1 4NS, United Kingdom

³⁸University of London, Royal Holloway and Bedford New College, Egham, Surrey TW20 0EX, United Kingdom

³⁹University of Louisville, Louisville, Kentucky 40292, USA

⁴⁰Johannes Gutenberg-Universität Mainz, Institut für Kernphysik, D-55099 Mainz, Germany

⁴¹University of Manchester, Manchester M13 9PL, United Kingdom

⁴²University of Maryland, College Park, Maryland 20742, USA

⁴³University of Massachusetts, Amherst, Massachusetts 01003, USA

⁴⁴Massachusetts Institute of Technology, Laboratory for Nuclear Science, Cambridge, Massachusetts 02139, USA

⁴⁵McGill University, Montréal, Québec, Canada H3A 2T8

⁴⁶INFN Sezione di Milano^a; Dipartimento di Fisica, Università di Milano^b, I-20133 Milano, Italy

⁴⁷University of Mississippi, University, Mississippi 38677, USA

⁴⁸Université de Montréal, Physique des Particules, Montréal, Québec, Canada H3C 3J7

⁴⁹INFN Sezione di Napoli^a; Dipartimento di Scienze Fisiche,
Università di Napoli Federico II^b, I-80126 Napoli, Italy

⁵⁰NIKHEF, National Institute for Nuclear Physics and High Energy Physics, NL-1009 DB Amsterdam, The Netherlands

⁵¹University of Notre Dame, Notre Dame, Indiana 46556, USA

⁵²Ohio State University, Columbus, Ohio 43210, USA

⁵³University of Oregon, Eugene, Oregon 97403, USA

⁵⁴INFN Sezione di Padova^a; Dipartimento di Fisica, Università di Padova^b, I-35131 Padova, Italy

- ⁵⁵Laboratoire de Physique Nucléaire et de Hautes Energies,
IN2P3/CNRS, Université Pierre et Marie Curie-Paris6,
Université Denis Diderot-Paris7, F-75252 Paris, France
- ⁵⁶INFN Sezione di Perugia^a; Dipartimento di Fisica, Università di Perugia^b, I-06100 Perugia, Italy
- ⁵⁷INFN Sezione di Pisa^a; Dipartimento di Fisica,
Università di Pisa^b; Scuola Normale Superiore di Pisa^c, I-56127 Pisa, Italy
- ⁵⁸Princeton University, Princeton, New Jersey 08544, USA
- ⁵⁹INFN Sezione di Roma^a; Dipartimento di Fisica,
Università di Roma La Sapienza^b, I-00185 Roma, Italy
- ⁶⁰Universität Rostock, D-18051 Rostock, Germany
- ⁶¹Rutherford Appleton Laboratory, Chilton, Didcot, Oxon, OX11 0QX, United Kingdom
- ⁶²CEA, Irfu, SPP, Centre de Saclay, F-91191 Gif-sur-Yvette, France
- ⁶³SLAC National Accelerator Laboratory, Stanford, California 94309 USA
- ⁶⁴University of South Carolina, Columbia, South Carolina 29208, USA
- ⁶⁵Southern Methodist University, Dallas, Texas 75275, USA
- ⁶⁶Stanford University, Stanford, California 94305-4060, USA
- ⁶⁷State University of New York, Albany, New York 12222, USA
- ⁶⁸Tel Aviv University, School of Physics and Astronomy, Tel Aviv, 69978, Israel
- ⁶⁹University of Tennessee, Knoxville, Tennessee 37996, USA
- ⁷⁰University of Texas at Austin, Austin, Texas 78712, USA
- ⁷¹University of Texas at Dallas, Richardson, Texas 75083, USA
- ⁷²INFN Sezione di Torino^a; Dipartimento di Fisica Sperimentale, Università di Torino^b, I-10125 Torino, Italy
- ⁷³INFN Sezione di Trieste^a; Dipartimento di Fisica, Università di Trieste^b, I-34127 Trieste, Italy
- ⁷⁴IFIC, Universitat de Valencia-CSIC, E-46071 Valencia, Spain
- ⁷⁵University of Victoria, Victoria, British Columbia, Canada V8W 3P6
- ⁷⁶Department of Physics, University of Warwick, Coventry CV4 7AL, United Kingdom
- ⁷⁷University of Wisconsin, Madison, Wisconsin 53706, USA

We study the process $e^+e^- \rightarrow J/\psi\pi^+\pi^-$ with initial-state-radiation events produced at the PEP-II asymmetric-energy collider. The data were recorded with the BABAR detector at center-of-mass energies 10.58 and 10.54 GeV, and correspond to an integrated luminosity of 454 fb^{-1} . We investigate the $J/\psi\pi^+\pi^-$ mass distribution in the region from 3.5 to 5.5 GeV/ c^2 . Below 3.7 GeV/ c^2 the $\psi(2S)$ signal dominates, and above 4 GeV/ c^2 there is a significant peak due to the Y(4260). A fit to the data in the range 3.74 – 5.50 GeV/ c^2 yields a mass value 4244 ± 5 (stat) ± 4 (syst) MeV/ c^2 and a width value 114^{+16}_{-15} (stat) ± 7 (syst) MeV for this state. We do not confirm the report from the Belle collaboration of a broad structure at 4.01 GeV/ c^2 . In addition, we investigate the $\pi^+\pi^-$ system which results from Y(4260) decay.

PACS numbers: 13.20.Gd, 13.25.Gv, 13.66.Bc, 14.40.Pq, 12.40.Yx, 12.39.Mk, 12.39.Pn, 12.39.Ki

1 The observation of the X(3872) [1], followed by the dis- 21
 2 covery of other states such as the $\chi_{c2}(2P)(3930)$ [2], the 22
 3 Y(3940) [3], and the X(3940) [4], has reopened interest 23
 4 in charmonium spectroscopy. These resonances cannot 24
 5 be fully explained by a simple charmonium model [5]. 25
 6 The Y(4260) was discovered [6] in the initial-state- 26
 7 radiation (ISR) process $e^+e^- \rightarrow \gamma_{\text{ISR}}Y(4260)$, $Y(4260) \rightarrow$ 27
 8 $J/\psi\pi^+\pi^-$. Since it is produced directly in e^+e^- annihi- 28
 9 lation, it has $J^{PC} = 1^{--}$. The observation of the decay 29
 10 mode $J/\psi\pi^0\pi^0$ [7] established that it has zero isospin. 30
 11 However it is not observed to decay to $D^*\bar{D}^*$ [8], nor 31
 12 to $D_s^*\bar{D}_s^*$ [9], so that its properties do not lend them- 32
 13 selves to a simple charmonium interpretation, and its 33
 14 nature is still unclear. Other interpretations, such as 34
 15 a four-quark state [10, 11], a baryonium state [12], or 35
 16 a hybrid state [13], have been proposed. However if 36
 17 the Y(4260) is a four-quark state it is expected to de- 37
 18 cay to $D_s^+\bar{D}_s^-$ [11], but this has not been observed [9]. 38
 19 An analysis of the reaction $e^+e^- \rightarrow J/\psi\pi^+\pi^-$ [14] 39
 20 which confirms the Y(4260), suggests the existence of 40

a broad state with mass $m = 4008 \pm 40^{+114}_{-28}$ MeV/ c^2
 and width $\Gamma = 226 \pm 44 \pm 87$ MeV. Two additional
 $J^{PC} = 1^{--}$ states, the Y(4360) and the Y(4660), have
 been reported in ISR production, but only in the reaction
 $e^+e^- \rightarrow \psi(2S)\pi^+\pi^-$ [15, 16].

In this paper we present an ISR study of the reaction
 $e^+e^- \rightarrow J/\psi\pi^+\pi^-$ in the center-of-mass (c.m.) energy
 (E_{cm}) range 3.5 – 5.5 GeV. In the $J/\psi\pi^+\pi^-$ mass re-
 gion below ~ 3.7 GeV/ c^2 the signal due to the decay
 $\psi(2S) \rightarrow J/\psi\pi^+\pi^-$ dominates. A detailed comparison to
 $\psi(2S)$ Monte Carlo (MC) simulation yields values of the
 cross section and partial width to e^+e^- . The high-mass
 tail of the $\psi(2S)$ MC distribution describes the data up
 to ~ 4 GeV/ c^2 quite well, and so we perform a maximum
 likelihood fit over the 3.74–5.50 GeV/ c^2 mass region in
 which the fit function consists of the incoherent superpo-
 sition of a nonresonant, decreasing exponential function
 describing the $J/\psi\pi^+\pi^-$ mass region above 3.74 GeV/ c^2
 and a Breit-Wigner (BW) function describing produc-
 tion and decay of the Y(4260). Non- J/ψ background is

41 treated by means of a simultaneous fit to the mass dis-
 42 tribution from the J/ψ sideband regions.

43 This analysis uses a data sample corresponding to
 44 an integrated luminosity of 454fb^{-1} , recorded by the
 45 *BABAR* detector at the SLAC PEP-II asymmetric-energy
 46 e^+e^- collider operating at c.m. energies 10.58 and 10.54
 47 GeV. The detector is described in detail elsewhere [17].
 48 Charged-particle momenta are measured with a tracking
 49 system consisting of a five-layer, double-sided silicon
 50 vertex tracker (SVT), and a 40-layer drift chamber (DCH),
 51 both of which are coaxial with the 1.5-T magnetic field
 52 of a superconducting solenoid. An internally reflect-
 53 ing ring-imaging Cherenkov detector, and specific ion-
 54 ization measurements from the SVT and DCH, provide
 55 charged-particle identification (PID). A CsI(Tl) electro-
 56 magnetic calorimeter (EMC) is used to detect and iden-
 57 tify photons and electrons, and muons are identified using
 58 information from the instrumented flux-return system.

59 We reconstruct events corresponding to the reaction
 60 $e^+e^- \rightarrow \gamma_{\text{ISR}} J/\psi \pi^+ \pi^-$, where γ_{ISR} represents a photon
 61 that is radiated from the initial state e^\pm , thus lowering
 62 the c.m. energy of the e^+e^- collision which produces the
 63 $J/\psi \pi^+ \pi^-$ system. We do not require observation of the
 64 ISR photon, since it is detectable in the EMC for only
 65 $\sim 15\%$ of the events. This is because the ISR photon is
 66 produced predominantly in a direction close to the e^+e^-
 67 collision axis, and as such is most frequently outside the
 68 fiducial region of the EMC.

69 We select events containing exactly four charged-
 70 particle tracks, and reconstruct J/ψ candidates via their
 71 decay to e^+e^- or $\mu^+\mu^-$. For each mode, at least
 72 one of the leptons must be identified on the basis
 73 of PID information. When possible, electron candi-
 74 dates are combined with associated photons in order
 75 to recover bremsstrahlung energy loss, and so improve
 76 the J/ψ momentum measurement. An $e^+e^- (\mu^+\mu^-)$
 77 pair with invariant mass within $(-75, +55) \text{ MeV}/c^2$
 78 $((-55, +55) \text{ MeV}/c^2)$ of the nominal J/ψ mass [18] is ac-
 79 cepted as a J/ψ candidate. We refer to the combination
 80 of these e^+e^- and $\mu^+\mu^-$ mass intervals as “the J/ψ signal
 81 region”. Each J/ψ candidate is subjected to a geometric
 82 fit in which the decay vertex is constrained to the e^+e^-
 83 interaction region. The χ^2 probability of this fit must be
 84 greater than 0.001. An accepted J/ψ candidate is kine-
 85 matically constrained to the nominal J/ψ mass [18] and
 86 combined with a candidate $\pi^+\pi^-$ pair in a geometric fit,
 87 which must yield a vertex- χ^2 probability greater than
 88 0.001.

89 The value of the missing-mass-squared recoiling
 90 against the $J/\psi \pi^+ \pi^-$ system must be in the range
 91 $(-0.50, +0.75) (\text{GeV}/c^2)^2$ in order to be consistent with
 92 the recoil of an ISR photon. We require also that the
 93 transverse component of the missing momentum be less
 94 than $2.25 \text{ GeV}/c$. If the ISR photon is detected in the
 95 EMC, its momentum vector is added to that of the
 96 $J/\psi \pi^+ \pi^-$ system in calculating the missing momentum.
 97

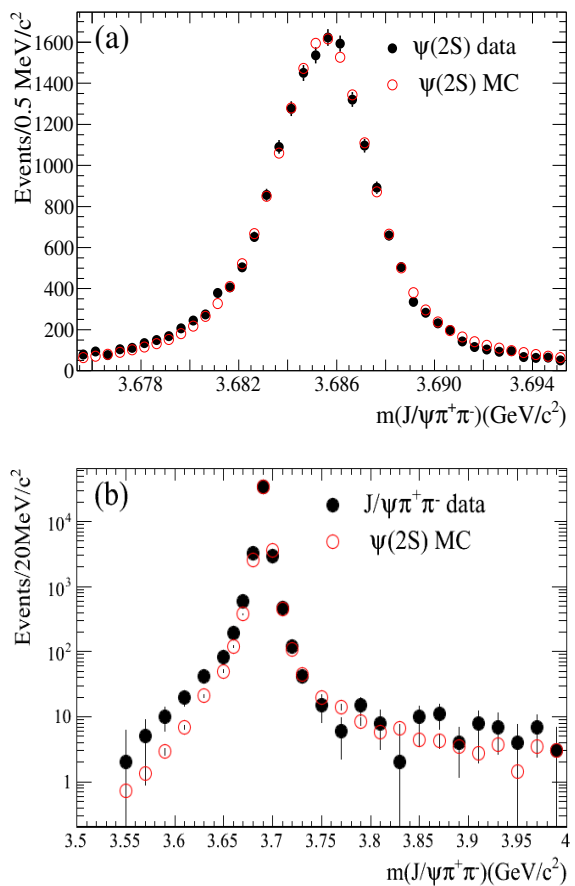


FIG. 1. (a) The background-subtracted data, and MC simulation modified as described in the text, for the $\psi(2S)$ peak region. (b) The corresponding distribution for the mass region below $4.0 \text{ GeV}/c^2$.

The candidate $\pi^+\pi^-$ system has a small contamination due to e^+e^- pairs from photon conversions. We compute the pair mass $m_{e^+e^-}$ with the electron mass assigned to each candidate pion, and remove events with $m_{e^+e^-} < 50 \text{ MeV}/c^2$. We estimate the remaining background by using events that have an $e^+e^- (\mu^+\mu^-)$ mass in the J/ψ sideband $(2.896, 2.971)$ or $(3.201, 3.256)$ ($(2.936, 2.991)$ or $(3.201, 3.256)$) GeV/c^2 after satisfying the other signal region selection criteria.

The $J/\psi \pi^+ \pi^-$ invariant-mass distribution in the region below $4 \text{ GeV}/c^2$ is dominated by the $\psi(2S)$ signal. The peak region, after subtraction of background from the J/ψ sideband regions, is shown in Fig. 1(a) (solid dots). The open dots indicate the $\psi(2S)$ MC distribution, modified as described below. The data distribution above $\sim 3.75 \text{ GeV}/c^2$ (Fig. 1(b)) may be due to the $\psi(2S)$ tail and a possible $J/\psi \pi^+ \pi^-$ continuum (*i.e.* non-resonant) contribution. In order to investigate this we performed a detailed comparison of the $\psi(2S)$ signal in data and in MC simulation. For the latter, we used the MC generator VECTORISR [19] and a simulation of the

119 *BABAR* detector based on Geant4 [20]. The resulting MC₁₇₅
 120 events were subjected to the reconstruction procedures₁₇₆
 121 which were applied to the data. 177

122 We first measured the peak mass position for both dis₁₇₈
 123 tributions. We performed a χ^2 -fit of a parabola to the₁₇₉
 124 data and MC distributions in intervals of 0.5 MeV/ c^2 ₁₈₀
 125 for the region within ± 5 MeV/ c^2 of the nominal $\psi(2S)$ ₁₈₁
 126 mass [18]. For the data, this gave a peak mass value₁₈₂
 127 of 3685.32 ± 0.02 (stat) MeV/ c^2 , which is 0.77 ± 0.04 ₁₈₃
 128 MeV/ c^2 less than the nominal value [18]. For the MC₁₈₄
 129 events, the result was 3685.43 ± 0.01 (stat) MeV/ c^2 ,₁₈₅
 130 which is 0.66 ± 0.01 MeV/ c^2 smaller than the input₁₈₆
 131 value [18]. This difference is attributed to final-state-₁₈₇
 132 radiation effects. The larger deviation obtained for data₁₈₈
 133 may result from under-estimated energy-loss corrections,₁₈₉
 134 and/or magnetic field uncertainty [21, 22]. Each MC₁₉₀
 135 event was then displaced by 0.11 MeV/ c^2 toward lower₁₉₁
 136 mass, and the parabolic fit to the new MC distribution₁₉₂
 137 was repeated. The MC distribution was normalized to₁₉₃
 138 the data by using the data-to-MC ratio of the maxima₁₉₄
 139 of the fitted functions. In order to improve the MC-₁₉₅
 140 data resolution agreement, a χ^2 function incorporating₁₉₇
 141 the data-MC histogram differences and their uncertain₁₉₈
 142 ties was created for the region within ± 10 MeV/ c^2 of the₁₉₉
 143 peak mass value. In the minimization procedure each₂₀₀
 144 MC event was represented in mass by a superposition₂₀₁
 145 of two Gaussian functions with a common center, but₂₀₂
 146 different fractional contributions, and normalized to one₂₀₃
 147 event. The root-mean-squared (r.m.s.) deviations of the₂₀₄
 148 Gaussian functions, and the fractional contribution of the₂₀₅
 149 narrower Gaussian function to the normalized distribu₂₀₆
 150 tion, were allowed to vary in the fit, and the contribution₂₀₇
 151 of each smeared MC event to each histogram interval₂₀₈
 152 was accumulated. This procedure yielded a new MC his₂₀₉
 153 togram to be used in the fit to the data histogram. We₂₁₀
 154 iterated the above procedure until the change in χ^2 was₂₁₁
 155 less than 0.1, at which point the narrow (broad) Gaussian₂₁₂
 156 r.m.s. deviation was 0.7 (6.3) MeV/ c^2 , and the fractional₂₁₃
 157 contribution was 0.88 (0.12). 214

158 In Fig. 1(a) the final MC distribution is compared to₂₁₅
 159 the data in the fit region, and the agreement is good₂₁₆
 160 ($\chi^2/\text{NDF} = 30.7/35$, probability = 67.6 %; NDF is the₂₁₇
 161 number of degrees of freedom). We integrate this MC₂₁₈
 162 distribution over the entire lineshape in order to esti₂₁₉
 163 mate the $\psi(2S)$ signal yield in data, and obtain 20893 ₂₂₀
 164 ± 145 (stat) events. We use the efficiency and the₂₂₁
 165 distributed luminosity (obtained from the nominal inte₂₂₂
 166 grated luminosity and the second-order radiator function₂₂₃
 167 from Ref. [23]) to obtain the cross section value $14.05 \pm$ ₂₂₄
 168 0.26 (stat) pb for radiative return to the $\psi(2S)$. This is₂₂₅
 169 in agreement with a previous measurement [14]. In ad₂₂₆
 170 dition we extract $\Gamma(\psi(2S) \rightarrow e^+e^-) = 2.31 \pm 0.05$ (stat)₂₂₇
 171 keV, in excellent agreement with Ref. [18]. 228

172 In Fig. 1(b) we compare the modified $\psi(2S)$ MC dis₂₂₉
 173 tribution to the data in the region below $4.0 \text{ GeV}/c^2$. The
 174 MC low-mass tail is systematically below the data distri-

tribution, but the high-mass tail provides a good descrip₂₃₀
 175 tion of the observed events. However, we note that the
 176 extrapolation to this region requires the use of the $\psi(2S)$
 177 Breit-Wigner lineshape at mass values which are as much
 178 as 1000 full-widths beyond the central mass. The exist₂₃₁
 179 ence of many other measured final state contributions
 180 to the $J^{PC} = 1^{--}$ amplitude in this mass region must
 181 call this procedure into question. Although our model
 182 adequately describes the data between the $\psi(2S)$ peak
 183 and $\sim 4.0 \text{ GeV}/c^2$, we cannot discount the possibility
 184 of a contribution from an $e^+e^- \rightarrow J/\psi \pi^+\pi^-$ continuum
 185 cross section in this region. In this regard, the failure of
 186 the MC lineshape to describe the data in the region of
 187 the low-mass tail might be due to the threshold rise of
 188 just such a continuum cross section.

The $J/\psi \pi^+\pi^-$ mass distribution corresponding to the
 189 J/ψ signal region is shown from 3.74 to 5.5 GeV/c^2 in
 190 Fig. 2(a). The shaded histogram, which has been ob₂₃₂
 191 tained by linear interpolation from the J/ψ sideband re₂₃₃
 192 gions, represents the estimated background contribution
 193 to the J/ψ signal region. The signal distribution shows
 194 an excess of events over background above 3.74 GeV/c^2
 195 which might result from the $\psi(2S)$ tail and a possible
 196 $J/\psi \pi^+\pi^-$ continuum contribution, as discussed with
 197 respect to Fig. 1(b). At higher mass we observe clear
 198 production of the $Y(4260)$, and beyond $\sim 4.8 \text{ GeV}/c^2$ the
 199 data are consistent with background only. There is a
 200 small excess of events near 4.5 GeV/c^2 , which we choose
 201 to attribute to statistical fluctuation. In this regard, we
 202 note that no corresponding excess is observed in Ref. [14].
 203 The background contribution is featureless throughout
 204 the mass region being considered.

In order to extract the parameter values of the
 205 $Y(4260)$, we perform an unbinned, extended-maximum-
 206 likelihood fit in the region 3.74–5.5 GeV/c^2 to the
 207 $J/\psi \pi^+\pi^-$ distribution from the J/ψ signal region, and
 208 simultaneously to the background distribution from the
 209 J/ψ sidebands. The background is fitted using a third-
 210 order polynomial in $J/\psi \pi^+\pi^-$ mass, m . The mass-
 211 dependence of the signal function is given by $f(m) =$
 212 $\epsilon(m) \cdot \mathcal{L}(m) \cdot \sigma(m)$, where $\epsilon(m)$ is the mass-dependent
 213 signal-selection efficiency from MC simulation with a
 214 $J/\psi \pi^+\pi^-$ phase space distribution, and $\mathcal{L}(m)$ is the
 215 mass-distributed luminosity [23], where we ignore the
 216 small corrections due to initial-state emission of addi₂₁₇
 217 tional soft photons; $\epsilon(m)$ increases from 9.5% at 3.74
 218 GeV/c^2 to 15.5% at 5.5 GeV/c^2 , and $\mathcal{L}(m)$ from 35
 219 $\text{pb}^{-1}/20 \text{ MeV}$ to $61.3 \text{ pb}^{-1}/20 \text{ MeV}$ over the same range.
 220 The cross section, $\sigma(m)$, is given by the incoherent sum
 221 $\sigma(m) = \sigma_{\text{NR}}(m) + \sigma_{\text{BW}}(m)$, where $\sigma_{\text{NR}}(m)$ is an expo₂₂₂
 222 nential function which provides an empirical description
 223 of the $\psi(2S)$ tail and possible continuum contributions;
 224 $\sigma_{\text{BW}}(m)$ is the cross section for the production of the

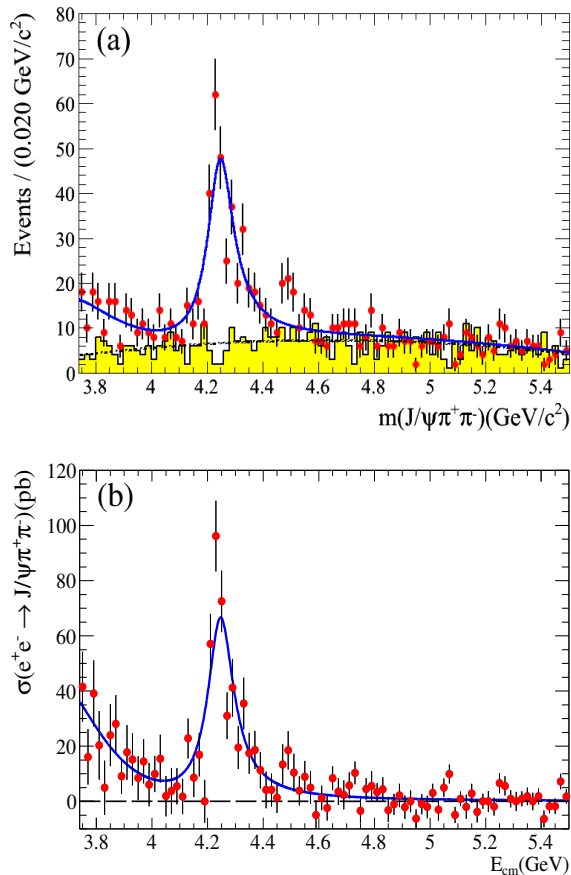


FIG. 2. (a) The $J/\psi\pi^+\pi^-$ mass spectrum from 3.74 GeV/c^2 to 5.5 GeV/c^2 ; the points represent the data and the shaded histogram is the background from the J/ψ sidebands; the solid curve represents the fit result, and the dashed curve results from the simultaneous fit to the background; (b) the measured $e^+e^- \rightarrow J/\psi\pi^+\pi^-$ cross section as a function of c.m. energy; the solid curve results from the fit shown in (a).

TABLE I. Systematic uncertainty estimates for the Y(4260) parameter values.

Source	$\Gamma_{e^+e^-} \cdot \mathcal{B}(\%)$	Mass (MeV/c^2)	Γ (MeV)
Fit procedure	$+1.5$ -0.5	$+0$ -1	$+2$ -1
Mass Scale	-	± 0.6	-
Mass resolution	-	-	± 1.5
MC dipion model	± 3.6	-	-
Decay angular momentum	± 3.6	± 3.5	± 7
Luminosity, etc. (see text)	± 5.4	-	-

tion which increases linearly from 2.1 MeV/c^2 at ~ 3.5 GeV/c^2 to 5 MeV/c^2 at ~ 4.3 GeV/c^2 . The results of the fit are shown in Fig. 2(a). The parameter values obtained for the Y(4260) are $m_Y = 4244 \pm 5$ (stat) MeV/c^2 , $\Gamma_Y = 114^{+16}_{-15}$ (stat) MeV, and $\Gamma_{e^+e^-} \times \mathcal{B}(J/\psi\pi^+\pi^-) = 9.2 \pm 0.8$ (stat) eV.

For each $J/\psi\pi^+\pi^-$ mass interval, i , we calculate the $e^+e^- \rightarrow J/\psi\pi^+\pi^-$ cross section after background subtraction using

$$\sigma_i = \frac{n_i^{\text{obs}} - n_i^{\text{bkg}}}{\epsilon_i \cdot \mathcal{L}_i \cdot \mathcal{B}(J/\psi \rightarrow l^+l^-)}, \quad (2)$$

with n_i^{obs} and n_i^{bkg} the number of observed and background events, respectively, for this interval; ϵ_i , and \mathcal{L}_i are the values of $\epsilon(m)$ and $\mathcal{L}(m)$ [23] at the center of interval i .

The resulting cross section is shown in Fig. 2(b), where the solid curve is obtained from the simultaneous likelihood fit. The corresponding estimates of systematic uncertainty are due to luminosity (1%), tracking (5.1%), $\mathcal{B}(J/\psi \rightarrow l^+l^-)$ (0.7%), efficiency (1%) and PID (1%); combined in quadrature. These yield a net systematic uncertainty of 5.4%, as indicated in Table I.

The reaction $e^+e^- \rightarrow J/\psi\pi^+\pi^-$ has been studied at the c.m. energy of the $\psi(3770)$ by the CLEO [24] and BES [25] collaborations. The former reported the value 12.1 ± 2.2 pb for the $e^+e^- \rightarrow \psi(3770) \rightarrow J/\psi\pi^+\pi^-$ cross section, after subtraction of the contribution resulting from radiative return to the $\psi(2S)$. The dependence on E_{cm} of our fitted cross section, shown by the curve in Fig. 2(b), yields the value 31 ± 5 (stat) ± 2 (syst) pb at the $\psi(3770)$ with no subtraction of a $\psi(2S)$ contribution. This is compatible with the much more precise CLEO result obtained after subtraction. No cross section value is reported in Ref. [25], but the results of the BES analysis agree within their significantly larger uncertainties with those from CLEO.

The systematic uncertainties on the measured values of the Y(4260) parameters include contributions from the fitting procedure (evaluated by changing the fit range and

Y(4260), and is given by

$$\sigma_{\text{BW}}(m) = \frac{12\pi C}{m^2} \cdot \frac{PS(m)}{PS(m_Y)} \cdot \frac{\Gamma_{e^+e^-} \cdot \mathcal{B}(J/\psi\pi^+\pi^-) \cdot m_Y^2 \cdot \Gamma_Y}{(m_Y^2 - m^2)^2 + m_Y^2 \Gamma_Y^2}, \quad (1)$$

where m_Y and Γ_Y are the mass and width of the Y(4260), $\Gamma_{e^+e^-}$ is the partial width for $Y(4260) \rightarrow e^+e^-$, $\mathcal{B}(J/\psi\pi^+\pi^-)$ is the branching fraction for $Y(4260) \rightarrow J/\psi\pi^+\pi^-$, and $C = 0.3894 \times 10^9$ GeV^2 pb. The function $PS(m)$ represents the mass dependence of $J/\psi\pi^+\pi^-$ phase space, and $PS(m_Y)$ is its value at the mass of the Y(4260). In the likelihood function, $\sigma_{\text{BW}}(m)$ is multiplied by $\mathcal{B}(J/\psi \rightarrow l^+l^-)$, the branching fraction sum of the e^+e^- and $\mu^+\mu^-$ decay modes [18], since the fit is to the observed events. In the fit procedure $f(m)$ is convolved with a Gaussian resolution function obtained from MC simulation. This function has a r.m.s. deviation

the background parametrization), the uncertainty in the mass scale, the mass-resolution function, and the change in efficiency when the dipion distribution is simulated using the solid histogram in Fig. 3(c), which is described below. In Eq. (1) it is assumed that $Y(4260)$ decay to a J/ψ and a scalar dipion occurs in an S -wave orbital angular momentum state. However, a D -wave decay between the J/ψ and the $\pi^+\pi^-$ system can occur also, and for this hypothesis the fitted central values of mass, width, and $\Gamma_{e^+e^-} \times \mathcal{B}(J/\psi \pi^+\pi^-)$ become $4237 \text{ MeV}/c^2$, 100 MeV , and 8.5 eV , respectively. We assign half the change in central value of each quantity as a conservative estimate of systematic uncertainty associated with the decay angular momentum. Uncertainties associated with luminosities, tracking, $\mathcal{B}(J/\psi \rightarrow l^+l^-)$, efficiency and PID affect only $\Gamma_{e^+e^-} \cdot \mathcal{B}$, and their net contribution is 5.4%, as we discussed previously. Our estimates of systematic uncertainty are summarized in Table I, and are combined in quadrature to obtain the values which we quote for the $Y(4260)$.

We now consider the $\pi^+\pi^-$ system from $Y(4260)$ decay to $J/\psi \pi^+\pi^-$. Since the $Y(4260)$ has $I(J^{PC}) = 0(1^{--})$ and its width indicates strong decay, the $\pi^+\pi^-$ system has $I(J^{PC}) = 0(0^{++})$ or $I(J^{PC}) = 0(2^{++})$. For the region $4.15 \leq m(J/\psi \pi^+\pi^-) \leq 4.45 \text{ GeV}/c^2$, the $\pi^+\pi^-$ mass distribution after subtraction of that from the J/ψ sideband regions is shown in Fig. 3(a). The region below $0.32 \text{ GeV}/c^2$ is excluded since it is severely depopulated by the procedure used to remove e^+e^- pair contamination. The distribution decreases from threshold to near zero at $\sim 0.6 \text{ GeV}/c^2$, rises steadily to a maximum at $\sim 0.95 \text{ GeV}/c^2$, decreases rapidly to near zero again at $\sim 1 \text{ GeV}/c^2$, and increases thereafter. The distribution is consistent with previous measurements [6, 14].

We define θ_π as the angle between the π^+ direction and that of the recoil J/ψ , both in the dipion rest frame. The distribution in $\cos\theta_\pi$ is shown in Fig. 3(b). The fitted line represents S -wave decay, and provides an adequate description of the data ($\chi^2/NDF = 12.3/9$, probability = 19.7%); there is no need for a D -wave contribution, *e.g.*, from $f_2(1270) \rightarrow \pi^+\pi^-$ decay.

The mass distribution near $1 \text{ GeV}/c^2$ suggests coherent addition of a nonresonant $\pi^+\pi^-$ amplitude and a resonant amplitude describing the $f_0(980)$. If the peak near $950 \text{ MeV}/c^2$ is attributed to a nonresonant amplitude with phase near 90° , the coherent addition of the resonant $f_0(980)$ amplitude, in the context of elastic unitarity, could result in the observed behavior, which is similar to that of the $I = 0 \pi^+\pi^-$ elastic scattering cross section near 1 GeV (Fig. 2, p.VII.38, of Ref. [26]). However, we have no phase information with which to support this conjecture.

The distribution in Fig. 3(a) for $m_{\pi\pi} < 0.9 \text{ GeV}/c^2$ is qualitatively similar to that observed for the decay $\Upsilon(3S) \rightarrow \Upsilon(1S)\pi^+\pi^-$ [27]. There, the dipion mass distribution decreases from a maximum near threshold to a

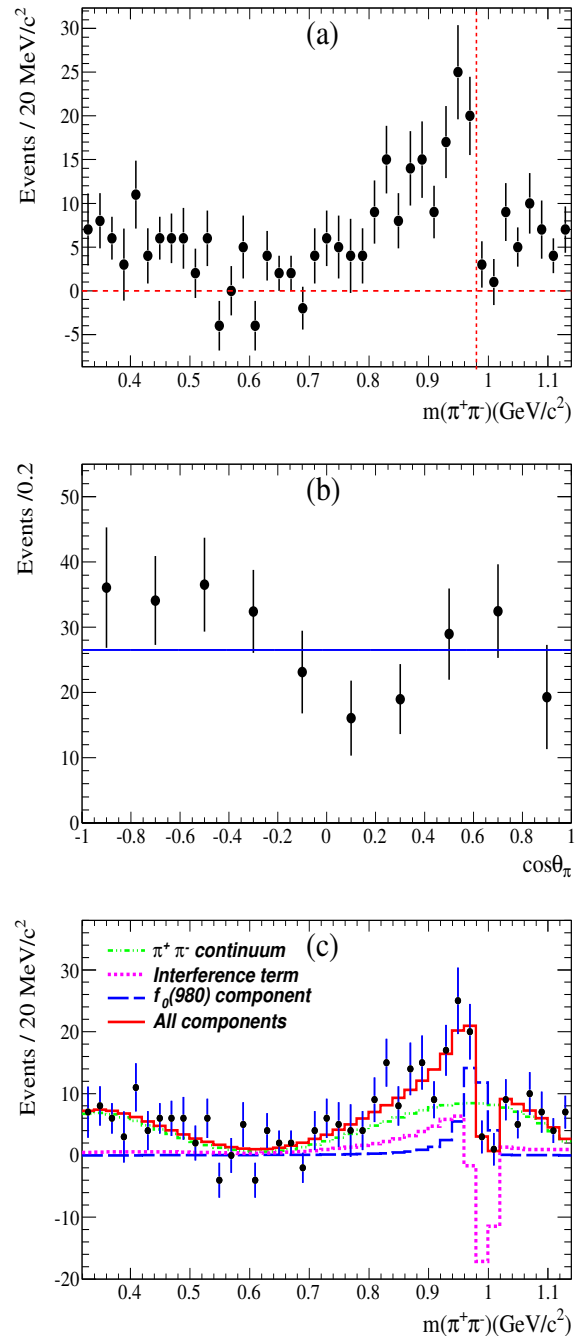


FIG. 3. (a) The background-subtracted $\pi^+\pi^-$ mass distribution for the $Y(4260)$ signal region; the dashed vertical line is at the nominal $f_0(980)$ mass value [18]; (b) the corresponding $\cos\theta_\pi$ distribution; the fitted line is for an S -wave description; (c) the result of the fit using the model of Eq. (3).

significantly non-zero minimum at $\sim 0.6\text{-}0.7 \text{ GeV}/c^2$, before rising steeply toward $0.8 \text{ GeV}/c^2$ before being cut-off by the kinematic limit ($0.895 \text{ GeV}/c^2$). The CLEO data are well-described in terms of a QCD multipole expansion [28, 29] up to $m_{\pi\pi} \sim 0.7 \text{ GeV}/c^2$, but the sharp rise thereafter is not well-accommodated. This shortcoming

is more readily apparent for the much larger *BABAR* data sample for this same process [30]. There the distribution begins a rapid rise toward the $f_0(980)$ region, but turns over at ~ 0.85 because of the kinematic limit at $0.895 \text{ GeV}/c^2$. The CLEO multipole expansion fit involves two amplitudes whose relative phase (± 155 degrees) causes destructive interference, and hence the minimum in the mass distribution at $\sim 0.6\text{--}0.7 \text{ GeV}/c^2$. The amplitudes are of similar magnitude in this region, and so a relative phase of ± 180 degrees could yield near-zero intensity, as observed in Fig. 3(a). This phase value would result in an approximately real amplitude. However it would contain no explicit $f_0(980)$ contribution, which seems necessary to describe the data of Fig. 3(a), and so we attempt to describe the entire distribution using the following simple model.

The nonresonant intensity distribution requires three turning points, as in the CLEO multipole expansion description, and so we choose to represent it by a fourth order polynomial, $T(m_{\pi\pi})$, where $m_{\pi\pi}$ is the invariant mass of the $\pi^+\pi^-$ system. From the phase requirement discussed above, it follows that the corresponding amplitude can be chosen to be real and represented by $\sqrt{T(m_{\pi\pi})}$. To this amplitude we add the complex S -wave $\pi^+\pi^-$ amplitude obtained from the *BABAR* analysis of $D_s^+ \rightarrow \pi^+\pi^-\pi^+$ decay [31], which shows clear resonant behavior at the $f_0(980)$. We perform a χ^2 -fit to the data of Fig. 3(a) using

$$f(m_{\pi\pi}) = |\sqrt{T(m_{\pi\pi})} + e^{i\phi} F_{f_0(980)}(m_{\pi\pi})|^2 \cdot p \cdot q, \quad (3)$$

where $F_{f_0(980)}$ is proportional to the complex $\pi^+\pi^-$ amplitude of Ref. [31], and the phase ϕ is determined by the fit; p is the π^+ momentum in the $\pi^+\pi^-$ rest frame, and q is the J/ψ momentum in the $J/\psi\pi^+\pi^-$ rest frame. We use the fitted $Y(4260)$ mass value in calculating q , which implies a kinematic limit of $1.15 \text{ GeV}/c^2$ for the fit function. The result is shown in Fig. 3(c). The fit is good ($\chi^2/NDF = 33.6/35$, probability = 53.6%), and the interference contribution is important for the description of the region near $1 \text{ GeV}/c^2$ ($\phi = 28^\circ \pm 24^\circ$). The $f_0(980)$ amplitude squared gives 0.17 ± 0.13 (stat) for the branching ratio $\mathcal{B}(J/\psi f_0(980), f_0(980) \rightarrow \pi^+\pi^-)/\mathcal{B}(J/\psi\pi^+\pi^-)$. This is somewhat smaller than the prediction of Ref. [32], where it is proposed that the $f_0(980)$ contribution should be dominant.

In summary, we have used ISR events to study the process $e^+e^- \rightarrow J/\psi\pi^+\pi^-$ in the c.m. energy range $3.74\text{--}5.50 \text{ GeV}$. For the $Y(4260)$ we obtain $m_Y = 4244 \pm 5$ (stat) ± 4 (syst) MeV/c^2 , $\Gamma_Y = 114^{+16}_{-15}$ (stat) ± 7 (syst) MeV , and $\Gamma_{e^+e^-} \times \mathcal{B}(J/\psi\pi^+\pi^-) = 9.2 \pm 0.8$ (stat) ± 0.7 (syst) eV . These results represent an improvement in statistical precision of $\sim 30\%$ over the previous *BABAR* results [6], and agree very well in magnitude and statistical precision with the

results of the Belle fit which uses a single Breit-Wigner resonance to describe the data [14]. We do not confirm the broad enhancement at $4.01 \text{ GeV}/c^2$ reported in Ref. [14]. The dipion system for the $Y(4260)$ decay is in a predominantly S -wave state. The mass distribution exhibits an $f_0(980)$ signal, for which a simple model indicates a branching ratio with respect to $J/\psi\pi^+\pi^-$ of 0.17 ± 0.13 (stat).

We are grateful for the excellent luminosity and machine conditions provided by our PEP-II colleagues, and for the substantial dedicated effort from the computing organizations that support *BABAR*. The collaborating institutions wish to thank SLAC for its support and kind hospitality. This work is supported by DOE and NSF (USA), NSERC (Canada), CEA and CNRS-IN2P3 (France), BMBF and DFG (Germany), INFN (Italy), FOM (The Netherlands), NFR (Norway), MES (Russia), MICINN (Spain), STFC (United Kingdom). Individuals have received support from the Marie Curie EIF (European Union) and the A. P. Sloan Foundation (USA).

* Now at the University of Tabuk, Tabuk 71491, Saudi Arabia

† Also with Università di Perugia, Dipartimento di Fisica, Perugia, Italy

‡ Now at the University of Huddersfield, Huddersfield HD1 3DH, UK

§ Now at University of South Alabama, Mobile, Alabama 36688, USA

¶ Also with Università di Sassari, Sassari, Italy

- [1] S. K. Choi *et al.*, Phys. Rev. Lett. **91**, 262001 (2003).
- [2] S. Uehara *et al.*, Phys. Rev. Lett. **96**, 082003 (2006).
- [3] S. K. Choi *et al.*, Phys. Rev. Lett. **94**, 182002 (2005).
- [4] K. Abe *et al.*, Phys. Rev. Lett. **98**, 082001 (2007).
- [5] T. Appelquist, R. M. Barnett and K. D. Lane, Ann. Rev. Nucl. Part. Sci. **28**, 387 (1978).
- [6] B. Aubert *et al.*, Phys. Rev. Lett. **95**, 142001 (2005).
- [7] T. E. Coan *et al.* Phys. Rev. Lett. **96**, 162003 (2006).
- [8] B. Aubert *et al.*, Phys. Rev. D **76**, 111105 (2007); B. Aubert *et al.*, Phys. Rev. D **79**, 092001 (2009); G. Pakhlova *et al.*, Phys. Rev. Lett. **98**, 092001 (2007); G. Pakhlova *et al.*, Phys. Rev. D **77**, 011103 (2008).
- [9] P. del Amo Sanchez *et al.*, Phys. Rev. D **82**, 052004 (2010); J. Libby *et al.*, Nucl. Phys. B, Proc. Suppl. **181-182**, 127 (2008).
- [10] I. Bigi *et al.*, Phys. Rev. D **72**, 114016 (2005).
- [11] L. Maiani *et al.*, Phys. Rev. D **72**, 031502 (2005).
- [12] C. -F. Qiao, J. Phys. G **35**, 075008 (2008).
- [13] S. -L. Zhu, Phys. Lett. B **625**, 212 (2005).
- [14] C. Z. Yuan *et al.*, Phys. Rev. Lett. **99**, 182004 (2007).
- [15] B. Aubert *et al.*, Phys. Rev. Lett. **98**, 212001 (2007).
- [16] X. L. Wang *et al.*, Phys. Rev. Lett. **99**, 142002 (2007).
- [17] B. Aubert *et al.*, Nucl. Instrum. Methods Phys. Res., Sect. A **479**, 1 (2002); W. Menges, IEEE Nucl. Sci. Symp. Conf. Rec. 5, 1470 (2006).
- [18] K. Nakamura *et al.*, J. Phys. G **37**, 075021 (2010), and partial update for the 2012 edition (URL:<http://pdg.lbl.gov>).

- 457 [19] G. Bonneau and F. Martin, Nucl. Phys. **B27**, 381 (1971);⁴⁶⁹
458 H.Czyz *et al.*, Eur. Phys. J. **C18**, 497 (2001); D. J. Lange,⁴⁷⁰
459 Nucl. Instrum. Methods Phys. Res., Sect. A **462**, 152⁴⁷¹
460 (2001).⁴⁷²
- 461 [20] S. Agostinelli *et al.*, Nucl. Instrum. Methods Phys. Res.,⁴⁷³
462 Sect. A **506**, 250 (2003).⁴⁷⁴
- 463 [21] B. Aubert *et al.*, Phys. Rev. D **80**, 092005 (2009).⁴⁷⁵
- 464 [22] B. Aubert *et al.*, Phys. Rev. D **72**, 052006 (2005).⁴⁷⁶
- 465 [23] E. A. Kuraev and V. S. Fadin, Sov. J. Nucl. Phys. **41**,⁴⁷⁷
466 466 (1985).⁴⁷⁸
- 467 [24] N. E. Adam *et al.*, Phys. Rev. Lett. **96**, 082004 (2006).⁴⁷⁹
- 468 [25] J. Z. Bai *et al.*, Phys. Lett. B **605**, 63 (2005).
- [26] K. Hikasa *et al.* Phys. Rev. D **45**, Part II (1992).
- [27] D. Cronin-Hennessy *et al.* Phys. Rev. D **76**, 072001
(2007).
- [28] L. S. Brown and R. N. Cahn, Phys. Rev. Lett. **35**, 1
(1975).
- [29] T. -M. Yahn, Phys. Rev. D **22**, 1652 (1980).
- [30] E. Guido, Ph.D. Thesis, Università degli Studi di Genova
(2011); *BABAR* Publications, THESIS-12/003 (2012).
- [31] B. Aubert *et al.*, Phys. Rev. D **79**, 032003 (2009).
- [32] A. Martinez Torres *et al.*, Phys. Rev. D **80**, 094012
(2009).